EXPLICIT AND IMPLICIT SOLUTIONS OF FIRST ORDER ALGORITHMS APPLIED TO THE EULER EQUATIONS IN TWO-DIMENSIONS

Edisson Sávio de Góes Maciel

*Mechanical Engineer/Researcher – Rua Demócrito Cavalcanti, 152 – Afogados – Recife –
Pernambuco – Brazil – 50750-080 – edissonsavio@yahoo.com.br*

Keywords: Flux difference splitting algorithms, Flux vector splitting algorithms, First order schemes, Explicit and implicit formulations, Euler equations.

Abstract. In this work, the Roe, the Steger and Warming, the Van Leer, the Chakravarthy and Osher, the Harten, the MacCormack, the Frink, Parikh and Pirzadeh, the Liou and Steffen Jr. and the Radespiel and Kroll first order schemes are implemented employing an implicit formulation to solve the Euler equations in the two-dimensional space. These schemes are implemented according to a finite volume formulation and using a structured spatial discretization. The Roe, the Chakravarthy and Osher, the Harten and the Frink, Parikh and Pirzadeh schemes are flux difference splitting ones, whereas the others are flux vector splitting schemes. The implicit schemes employ an ADI ("Alternating Direction Implicit") approximate factorization or Symmetric Line Gauss-Seidel to solve implicitly the Euler equations. Explicit and implicit results are compared, as also the computational costs, trying to emphasize the advantages and disadvantages of each formulation. The schemes are accelerated to the steady state solution using a spatially variable time step, which has demonstrated effective gains in terms of convergence rate according to Maciel. The algorithms are applied to the solution of the physical problem of the moderate supersonic flow along a compression corner. The results have demonstrated that the most accurate solutions are obtained with the Harten first order scheme, when implemented in its explicit version. The best wall pressure distribution is obtained by the Radespiel and Kroll first order scheme, in both explicit and implicit cases.

1   INTRODUCTION

Conventional non-upwind algorithms have been used extensively to solve a wide variety of problems (Kutler, 1975). Conventional algorithms are somewhat unreliable in the sense that for every different problem (and sometimes, every different case in the same class of problems) artificial dissipation terms must be specially tuned and judicially chosen for convergence. Upwind schemes are in general more robust but are also more involved in their derivation and application. Some authors proposed first order upwind schemes applied to the Euler equations, namely:

Roe (1981) presented a work that emphasized that several numerical schemes to the solution of the hyperbolic conservation equations were based on exploring the information obtained in the solution of a sequence of Riemann problems. It was verified that in the existent schemes the major part of these information was degraded and that only certain solution aspects were solved. It was demonstrated that the information could be preserved by the construction of a matrix with a certain "U property". After the construction of this matrix, its eigenvalues could be considered as wave velocities of the Riemann problem and the U_L-U_R projections over the matrix's eigenvectors would be the jumps between intermediate stages.

Steger and Warming (1981) used the remarkable property that the nonlinear flux vectors of the inviscid gasdynamic equations in conservation law form are homogeneous functions of degree one of the vector of conserved variables to develop their algorithm. This property readily permitted the splitting of the flux vectors into subvectors by similarity transformations so that each subvector had associated with it a specified eigenvalue spectrum. As a consequence of flux vector splitting, new explicit and implicit dissipative finite-difference schemes were developed for first-order hyperbolic systems of equations.

Van Leer (1982) suggested an upwind scheme based on the flux vector splitting concept. This scheme considered the fact that the convective flux vector components could be written as flow Mach number polynomial functions, as main characteristic. Such polynomials presented the particularity of having the minor possible degree and the scheme had to satisfy seven basic properties to form such polynomials.

Chakravarthy and Osher (1983) presented an upwind, shock capturing algorithm generalized to arbitrary coordinate systems. It could be applied to essentially all hyperbolic systems of conservation laws arising in physics, but became especially simple for the Euler equations. The method did not require any special properties of the Euler equations such as homogeneity. The Chakravarthy and Osher (1983) scheme is based on a Riemann problem solver, where compression waves are used to approximate shocks, resulting in cleaner results.

Harten (1983) developed a class of new finite difference schemes, explicit and with second order of spatial accuracy for calculation of weak solutions of the hyperbolic conservation laws. These highly nonlinear schemes were obtained by the application of a first order non-oscillatory scheme to an appropriately modified flux function. These second order algorithms reached high resolution, while preserving the robustness of the original scheme.

MacCormack (1985) developed a new implicit algorithm to solve the Euler and Navier-Stokes equations in two-dimensions. Techniques like line Gauss-Seidel and Newton iteration were implemented and tested aiming to accelerate the convergence of the numerical scheme. The calculation of viscous flow solutions at high Reynolds number in less than twenty time step iterations was demonstrated.

Frink, Parikh and Pirzadeh (1991) proposed a new scheme, unstructured and upwind, to the solution of the Euler equations. They tested the precision and the utility of this scheme in the analysis of the inviscid flows around two airplane configurations: one of transport

configuration, with turbines under the wings, and the other of high speed civil configuration. Tests were accomplished at subsonic and transonic Mach numbers with the transport airplane and at transonic and low supersonic Mach numbers with the civil airplane, yielding good results.

Liou and Steffen Jr. (1993) proposed a new flux vector splitting scheme. They declared that their scheme was simple and its accuracy was equivalent and, in some cases, better than the Roe (1981) scheme accuracy in the solutions of the Euler and the Navier-Stokes equations. The scheme was robust and converged solutions were obtained so fast as the Roe (1981) scheme. The authors proposed the approximated definition of an advection Mach number at the cell face, using its neighbor cell values via associated characteristic velocities. This Mach number was used to determine the upwind extrapolation of the convective quantities.

Radespiel and Kroll (1995) emphasized that the Liou and Steffen Jr. (1993) scheme had its merits of low computational complexity and low numerical diffusion as compared to other methods. They also mentioned that the original method had several problems. The method yielded local pressure oscillations in the shock wave proximities, adverse mesh and flow alignment difficulties. In the Radespiel and Kroll (1995) work, a hybrid scheme, which alternated between the Liou and Steffen Jr. (1993) and the Van Leer (1982) schemes, in the shock wave regions, was proposed, assuring that strength shocks were clear and well defined.

Traditionally, implicit numerical methods have been praised for their improved stability and condemned for their large arithmetic operation counts (Beam and Warming, 1978). On the one hand, the slow convergence rate of explicit methods become they so unattractive to the solution of steady state problems due to the large number of iterations required to convergence, in spite of the reduced number of operation counts per time step in comparison with their implicit counterparts. Such problem is resulting from the limited stability region which such methods are subjected (the Courant condition). On the other hand, implicit schemes guarantee a larger stability region, which allows the use of CFL numbers above 1.0, and fast convergence to steady state conditions. Undoubtedly, the most significant efficiency achievement for multidimensional implicit methods was the introduction of the Alternating Direction Implicit (ADI) algorithms by Douglas (1955), Peaceman and Rachford (1955), and Douglas and Gunn (1964). ADI approximate factorization methods consist in approximating the Left Hand Side (LHS) of the numerical scheme by the product of one-dimensional parcels, each one associated with a different spatial direction, which retract nearly the original implicit operator. These methods have been largely applied in the CFD community and, despite the fact of the error of the approximate factorization, it allows the use of large time steps.

In this work, the Roe (1981), the Steger and Warming (1981), the Van Leer (1982), the Chakravarthy and Osher (1983), the Harten (1983), the MacCormack (1985), the Frink, Parikh and Pirzadeh (1991), the Liou and Steffen Jr. (1993) and the Radespiel and Kroll (1995) first order schemes are implemented employing an implicit formulation to solve the Euler equations in two-dimensions. These schemes are implemented according to a finite volume formulation and using a structured spatial discretization. The Roe (1981), the Chakravarthy and Osher (1983), the Harten (1983) and the Frink, Parikh and Pirzadeh (1991) schemes are flux difference splitting ones, whereas the others are flux vector splitting schemes. The implicit schemes employ an ADI approximate factorization or Symmetric Line Gauss-Seidel to solve implicitly the Euler equations. Explicit and implicit results are compared, as also the computational costs, trying to emphasize the advantages and disadvantages of each formulation. The schemes are accelerated to the steady state solution using a spatially variable time step, which has demonstrated effective gains in terms of convergence rate (Maciel, 2005). The algorithms are applied to the solution of the physical

problem of the supersonic flow along a compression corner. The results have demonstrated that the most accurate solutions are obtained with the Harten (1983) first order scheme, when implemented in its explicit version. The best wall pressure distribution is obtained by the Radespiel and Kroll (1995) first order scheme, in both explicit and implicit cases.

2 EULER EQUATIONS

The fluid movement is described by the Euler equations, which express conservation of mass, of the linear momentum and of the energy to an inviscid mean, heat non-conductor and compressible, in the absence of external forces. These equations can be represented, in the integral and conservative forms, to a finite volume formulation, by:

$$\partial/\partial t \int_V Q dV + \int_S \left[E n_x + F n_y \right] dS = 0, \tag{1}$$

where Q is written to a Cartesian system, V is the cell volume, n_x and n_y are components of the normal unit vector to the flux face, S is the flux area, and E and F are components of the convective flux vector. The Q, E and F vectors are represented by:

$$Q = \{\rho \quad \rho u \quad \rho v \quad e\}^T, \quad E = \{\rho u \quad \rho u^2 + p \quad \rho u v \quad (e+p)u\}^T, \quad F = \{\rho v \quad \rho u v \quad \rho v^2 + p \quad (e+p)v\}^T, \tag{2}$$

with ρ being the fluid density; u and v are Cartesian components of the velocity vector in the x and y directions, respectively; e is the total energy; and p is the static pressure. The Euler equations were nondimensionalized in relation to the freestream density, ρ_∞, and in relation to the freestream speed of sound, a_∞, to the studied problem in this work. The matrix system of the Euler equations is closed with the state equation of a perfect gas

$$p = (\gamma - 1)\left[e - 0.5\rho(u^2 + v^2)\right]. \tag{3}$$

γ is the ratio of specific heats. The total enthalpy is determined by $H = (e+p)/\rho$.

3 NUMERICAL ALGORITHMS

The Roe (1981), the Steger and Warming (1981), the Van Leer (1982), the Harten (1983), the Frink, Parikh and Pirzadeh (1991), the Liou and Steffen Jr. (1993) and the Radespiel and Kroll (1995) first order schemes are described in details in Maciel (2008a,b), on a finite volume context. The Roe (1981), the Van Leer (1982), the Harten (1983), the Liou and Steffen Jr. (1993) and the Radespiel and Kroll (1995) schemes employ a time splitting method to explicit time integration (Maciel, 2008a,b). The Steger and Warming (1981) scheme employs a explicit Euler method (Maciel, 2008a) and the Frink, Parikh and Pirzadeh (1991) scheme employs a Runge-Kutta method of five stages (Maciel, 2008b) to explicit time integration. In this work, only the numerical flux vector of these schemes is presented:

3.1 Roe (1981) algorithm

The Roe (1981) dissipation function at the (i+1/2,j) interface is defined by:

$$\{D_{Roe}\}_{i+1/2,j} = [R]_{i+1/2,j} \{-\psi\alpha\}_{i+1/2,j}, \tag{4}$$

where R, ψ and α are described in Maciel (2008a). The numerical flux vector at the (i+1/2,j) interface is described by:

$$F^{(l)}_{i+1/2,j} = \left(E^{(l)}_{int} h_x + F^{(l)}_{int} h_y\right) V_{int} + 0.5 D^{(l)}_{Roe}, \tag{5}$$

with $E_{int}^{(l)}$, $F_{int}^{(l)}$, h_x, h_y and V_{int} calculated as indicated in Maciel (2008a,b); and "l" varies from 1 to 4 in two-dimensions.

3.2 Steger and Warming (1981) algorithm

The Steger and Warming (1981) numerical flux vector uses the following normal flux projection:

$$\widetilde{F}_{\pm}^{(n)} = \frac{\rho}{2\gamma}\left\{\begin{array}{c} \alpha \\ \alpha u + a\left(\lambda_2^{\pm} - \lambda_3^{\pm}\right)n_x \\ \alpha v + a\left(\lambda_2^{\pm} - \lambda_3^{\pm}\right)n_y \\ \alpha\dfrac{u^2 + v^2}{2} + av_n\left(\lambda_2^{\pm} - \lambda_3^{\pm}\right) + a^2\dfrac{\lambda_2^{\pm} + \lambda_3^{\pm}}{\gamma - 1} \end{array}\right\}, \tag{6}$$

where the eigenvalues of the normal Jacobian matrix are defined as

$$\lambda_1 = \vec{v} \bullet \vec{n} \equiv v_n, \quad \lambda_2 = \vec{v} \bullet \vec{n} + a \quad \text{and} \quad \lambda_3 = \vec{v} \bullet \vec{n} - a, \tag{7}$$

with $\vec{v}$ being the flow velocity vector, a is the speed of sound, $\pm$ sign indicates the positive or negative parts of the projection flux vector and of the eigenvalues; and α is defined in Maciel (2008a). The eigenvalue separation is defined to the ξ direction, for example, as:

$$\left(\lambda_{\xi}^l\right)^{\pm} = 0.5\left(\lambda_{\xi}^l \pm \left|\lambda_{\xi}^l\right|\right). \tag{8}$$

The numerical flux vectors of the Steger and Warming (1981) scheme, based on a finite volume formulation, are, for instance, calculated as:

$$\widetilde{F}_{i+1/2,j} = \left(\widetilde{F}_{i+1,j}^{-} + \widetilde{F}_{i,j}^{+}\right)S_{i+1/2,j} \quad \text{and} \quad \widetilde{F}_{i,j+1/2} = \left(\widetilde{F}_{i,j+1}^{-} + \widetilde{F}_{i,j}^{+}\right)S_{i,j+1/2}, \tag{9}$$

where S is the flux area described in Maciel (2008a,b).

3.3 Van Leer (1982) algorithm

The residual of the Van Leer (1982) scheme at the (i+1/2,j) interface is defined as:

$$R_{i+1/2,j}^e = |S|_{i+1/2,j}\left\{\frac{1}{2}M_{i+1/2,j}\left(\begin{bmatrix} \rho a \\ \rho au \\ \rho av \\ \rho aH \end{bmatrix}_L + \begin{bmatrix} \rho a \\ \rho au \\ \rho av \\ \rho aH \end{bmatrix}_R\right) - \frac{1}{2}\phi_{i+1/2,j}\left(\begin{bmatrix} \rho a \\ \rho au \\ \rho av \\ \rho aH \end{bmatrix}_R - \begin{bmatrix} \rho a \\ \rho au \\ \rho av \\ \rho aH \end{bmatrix}_L\right) + \begin{Bmatrix} 0 \\ S_x p \\ S_y p \\ 0 \end{Bmatrix}\right\}_{i+1/2,j}, \tag{10}$$

with R [cell (i+1,j)] and L [cell (i,j)] related to right and left states, S, S_x and S_y defining the flux area and its x and y components, a is the speed of sound, M is the Mach number splitting, ϕ is the dissipation function which defines the particular numerical scheme (an hybrid method based on the Van Leer, 1982, and the Liou and Steffen Jr., 1993, schemes), and the superscript "e" defines Euler equations. All these quantities are defined in Maciel (2008a,b). The definition of the ϕ dissipation term which determines the Van Leer (1982) scheme, according to Radespiel and Kroll (1995), is described as follows.

$$\phi_{i+1/2,j} = \phi_{i+1/2,j}^{VL} = \begin{cases} \left| M_{i+1/2,j} \right|, & if \ \left| M_{i+1/2,j} \right| \geq 1; \\ \left| M_{i+1/2,j} \right| + 0.5(M_R - 1)^2, & if \ 0 \leq M_{i+1/2,j} < 1; \\ \left| M_{i+1/2,j} \right| + 0.5(M_L + 1)^2, & if \ -1 < M_{i+1/2,j} \leq 0; \end{cases} \qquad (11)$$

3.4 Chakravarthy and Osher (1983) algorithm

Eigenvalues. The Jacobian matrices in generalized coordinates, necessary to define the system's eigenvalues according to the Chakravarthy and Osher (1983) scheme, are defined by:

$$\hat{A}_{i+1/2,j} = \left(h_x A + h_y B \right)_{i+1/2,j} \quad and \quad \hat{B}_{i,j+1/2} = \left(h_x A + h_y B \right)_{i,j+1/2}, \qquad (12)$$

where $A = \partial E / \partial Q$ and $B = \partial F / \partial Q$ are the Cartesian Jacobian matrices. Remembering that the sound speed is determined by $a = \sqrt{\gamma p / \rho}$, the eigenvalues of $\hat{A}$ are defined by:

$$\lambda_1 = (U + a)h_n, \ \lambda_{2,3} = Uh_n \quad and \quad \lambda_4 = (U - a)h_n, \qquad (13)$$

with $U = h_x' u + h_y' v$ and h_x' and h_y' defined in Maciel (2008a,b).

Riemann invariants. Riemann invariants are the building blocks for the Chakravarthy and Osher (1983) algorithm applied to Euler equations. Riemann invariants are associated with the eigenvalues of the generalized Jacobian matrices and are obtained from the corresponding right eigenvectors. For the Chakravarthy and Osher (1983) scheme, the Riemann invariants ψ corresponding to the *l*th eigenvalue are obtained by solving

$$\nabla_Q \psi \cdot r_l(Q) = 0, \qquad (14)$$

where ∇_Q is the gradient operator with respect to the vector of dependent variables denoted by Q and r_l is the *l*th right eigenvector. It may easily be verified that the following are Riemann invariants:

For $\lambda_1 = (U + a)h_n$:

$$\psi_2^1 = U - 2a/(\gamma - 1), \ \psi_3^1 = p/\rho^\gamma = S = \text{entropy} \quad and \quad \psi_4^1 = vh_x' - uh_y' = V; \qquad (15)$$

For $\lambda_{2,3} = Uh_n$:

$$\psi_1^{2,3} = p \quad and \quad \psi_4^{2,3} = U; \qquad (16)$$

For $\lambda_4 = (U - a)h_n$:

$$\psi_1^4 = U + 2a/(\gamma - 1), \ \psi_2^4 = p/\rho^\gamma = S = \text{entropy} \quad and \quad \psi_3^4 = vh_x' - uh_y' = V. \qquad (17)$$

The superscript denotes the eigenvalue to which the Riemann invariants correspond.

Intermediate states. In finite volumes the variable of interest are defined at the (i,j) cell centroid, where the vector of conserved variables is denoted as $Q_{i,j}$. The coordinate direction ξ is treated in details in this work and the extension to the η coordinate is straightforward. By simplicity, the index *j* is suppressed in the present notation.

Conventional finite volume schemes employ values at the cell centroids of the conserved variables, or dependents, of a simple manner. Such schemes are generally symmetric, what simplify their numerical implementation. The Chakravarthy and Osher (1983) algorithm is

more sophisticated. Fundamental to the Chakravarthy and Osher (1983) scheme are the intermediate states of the dependent variables, which are defined from the values of the cell states of the computational domain. While states in the computational cells are defined by Q_{i-1}, Q_i, etc., the correspondent intermediate states are defined by $Q_{i-2/3}$ and $Q_{i-1/3}$. The rest of this sublevel describes how these intermediate states are defined and their meanings.

Figure 1 serves as a guide to the construction of the intermediate values. The states *i-1* and *i* are connected through a curve in the state space which is made up of three subpaths. The first path connects Q_{i-1} and $Q_{i-2/3}$ and is associated with λ_1.
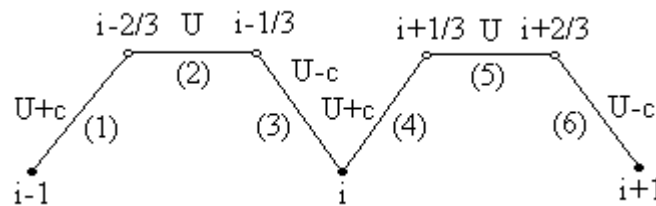
Figure 1: Schematic Representation of Chakravarthy and Osher (1983) Scheme in Terms of Intermediate and Cell Values of Dependent Variables.

Path 2 connecting $Q_{i-2/3}$ and $Q_{i-1/3}$ is associated with $\lambda_{2,3}$ and path 3 connecting $Q_{i-1/3}$ and Q_i is associated with λ_4. Thus $\psi^1_{2,3,4}$ are constant between Q_{i-1} and $Q_{i-2/3}$; $\psi^{2,3}_{1,4}$ are constant between $Q_{i-2/3}$ and $Q_{i-1/3}$; and $\psi^4_{1,2,3}$ are constant between $Q_{i-1/3}$ and Q_i. Equating Riemann invariants between the end points of each subpath it is possible to find $3+2+3 = 8$ equations to obtain the 8 unknown values of $Q_{i-2/3}$ and $Q_{i-1/3}$ from the known values at Q_{i-1} and Q_i. Thus the dependent variables at *i-2/3* and *i-1/3* are defined by the following formulas:

$$\rho_{i-1/3}^{(\gamma-1)/2} = \left[(\gamma-1)(U_i - U_{i-1})/2 + a_i + a_{i-1}\right]\Big/\left[a_i\left[1 + (S_{i-1}/S_i)^{1/(2\gamma)}\right]\right]\rho_i^{(\gamma-1)/2}; \qquad (18)$$

$$\rho_{i-1/3}^{(\gamma-1)/2} = \left[(\gamma-1)(U_i - U_{i-1})/2 + a_i + a_{i-1}\right]\Big/\left[a_{i-1}\left[1 + (S_i/S_{i-1})^{1/(2\gamma)}\right]\right]\rho_{i-1}^{(\gamma-1)/2}; \qquad (19)$$

$$p_{i-2/3} = p_{i-1/3} = S_{i-1}\rho_{i-2/3}^{\gamma}; \qquad (20)$$

$$U_{i-2/3} = U_{i-1} - 2/(\gamma-1)(a_{i-1} - a_{i-2/3}) = U_{i-1/3} = U_i + 2/(\gamma-1)(a_i - a_{i-1/3}); \qquad (21)$$

$$V_{i-2/3} = V_{i-1} \quad \text{and} \quad V_{i-1/3} = V_i. \qquad (22)$$

Once $Q_{i-1/3}$ and $Q_{i-2/3}$ are known, λ_1 may be computed at *i-1* and *i-2/3* and λ_4 at *i* and *i-1/3*. It can be shown that λ_1 and λ_4 can at most change sign only once along paths 1 and 3, respectively. If these eigenvalues do indeed change sign [if $\lambda_1(i-1)\cdot\lambda_1(i-2/3) < 0$, for example], it becomes necessary to compute the dependent variables at the points along paths 1 and 4 where the respective eigenvalues λ_1 and λ_4 vanish. These "sonic" points are defined as $\overline{Q}_{i-2/3}$ and $\overline{Q}_{i-1/3}$ and are given by the formulas that follow below:

$$\overline{U}_{i-1/3} = (\gamma-1)/(\gamma+1)(U_i + 2/(\gamma-1)a_i), \ \overline{\rho}_{i-1/3}^{(\gamma-1)/2} = \overline{U}_{i-1/3}/(\gamma S_i)^{1/2}; \qquad (23)$$

$$\overline{p}_{i-1/3} = S_i\overline{\rho}_{i-1/3}^{\gamma}, \ \overline{V}_{i-1/3} = V_i; \qquad (24)$$

$$\overline{U}_{i-2/3} = (\gamma-1)/(\gamma+1)(U_{i-1} - 2/(\gamma-1)a_{i-1}), \ \overline{\rho}_{i-2/3}^{(\gamma-1)/2} = -\overline{U}_{i-2/3}/(\gamma S_{i-1})^{1/2}; \qquad (25)$$

$$\overline{p}_{i-2/3} = S_{i-1}\overline{\rho}_{i-2/3}^{\gamma}, \ \overline{V}_{i-2/3} = V_{i-1}. \qquad (26)$$

Along path 2, the Riemann invariant $\psi^{2,3}_4$ is equal to λ_2/h_n. Thus λ_2 does not change either

magnitude or sign. The λ_1 and λ_4 fields are called genuinely nonlinear and the fields corresponding to $\lambda_{2,3}$ are termed linearly degenerate.

In Equations (21) and (22), (23) and (24) and (25) and (26), it is straightforward to decode for u and v from U and V (in generalized coordinates, U and V would be the normalized velocity contravariants). From these definitions, it is possible to write for u and v:

$$\begin{pmatrix} u \\ v \end{pmatrix} = \begin{bmatrix} h_x^{'} & -h_y^{'} \\ h_y^{'} & h_x^{'} \end{bmatrix} \begin{pmatrix} U \\ V \end{pmatrix}. \tag{27}$$

Paths of integration. In this sublevel, the values of the variables of the intermediate states and the values of the dependent variables at the cells of the computational domain are employed to form the Chakravarthy and Osher (1983) algorithm to the Euler equations. Initially, the net numerical flux vector in the ξ direction is approximated by:

$$F_{i+1/2,j} - F_{i-1/2,j} \approx \left[\int_{Q_{i-1}}^{Q_i} X\hat{A}dQ + \int_{Q_i}^{Q_{i+1}} (I - X)\hat{A}dQ \right]. \tag{28}$$

The matrix *X(Q)* and the paths of integration are what define the scheme. The subpaths of integration were recently defined (curves 1-3 of Fig. 1). The matrix *X(Q)* is defined to be:

$$X(Q) = R(Q)diag\left\{1/2 + 1/2 signal\left[\lambda_l(Q)\right]\right\}R^{-1}(Q), \tag{29}$$

where *R(Q)* is the right-eigenvector matrix or the matrix of column eigenvectors of the Jacobian matrix in generalized coordinates $\hat{A}$ and *R⁻¹(Q)* its inverse. Hence,

$$X\hat{A} = Rdiag\left[\max(\lambda_l,0)\right]R^{-1} = \hat{A}^+ \quad \text{and} \quad (I - X)\hat{A} = Rdiag\left[\min(\lambda_l,0)\right]R^{-1} = \hat{A}^-. \tag{30}$$

The asymmetric (upwind) character of the scheme is apparent from this definition. The Equation (28) can be more simplified by the partition of the original integration interval through the subpaths of integration:

$$\left|\int_{Q_{i-1}}^{Q_i} X\hat{A}dQ + \int_{Q_i}^{Q_{i+1}} (I - X)\hat{A}dQ\right| = F^{(n)}(h,Q_{i+1}) - F^{(n)}(h,Q_i) + \int_{i-1}^{i-2/3} \hat{A}^+ dQ + \int_{i-2/3}^{i-1/3} \hat{A}^+ dQ + \int_{i-1/3}^{i} \hat{A}^+ dQ$$
$$- \int_{i}^{i+1/3} \hat{A}^+ dQ - \int_{i+1/3}^{i+2/3} \hat{A}^+ dQ - \int_{i+2/3}^{i+1} \hat{A}^+ dQ, \tag{31}$$

with the normal flux to the interface defined by:

$$F^{(n)}(h,Q) = V_{\text{int}}\left\{\rho Uh_n \quad \rho uUh_n + ph_x \quad \rho vUh_n + ph_y \quad (e+p)Uh_n\right\}^T. \tag{32}$$

It is obvious so that the blocks of construction of the Chakravarthy and Osher (1983) scheme are the subintegrals along the subpaths connecting all pair of neighbor cells. To the interval between the pair of cells i-1 and i, for example, it is possible to define:

$$D1 = \int_{Q_{i-1}}^{Q_{i-2/3}} \hat{A}^+ dQ, \quad D2 = \int_{Q_{i-2/3}}^{Q_{i-1/3}} \hat{A}^+ dQ \quad \text{and} \quad D3 = \int_{Q_{i-1/3}}^{Q_i} \hat{A}^+ dQ. \tag{33}$$

While the integral formulae in the above equations seem very complex to be evaluated, they simplify considerably and each subintegral is reduced to the flux difference $F^{(n)}(Q)$ in each mesh cell and in each cell of the intermediate and sonic states. Therefore, it is possible to write:

$$D1 = F^{(n)}(h,Q_{i-2/3}) - F^{(n)}(h,Q_{i-1}), \text{if } \lambda_1(Q_{i-1}) > 0 \text{ and } \lambda_1(Q_{i-2/3}) > 0; \tag{34}$$

$$D1 = F^{(n)}(h, Q_{i-2/3}) - F^{(n)}(h, \overline{Q}_{i-2/3}), \text{ if } \lambda_1(Q_{i-1}) \le 0 \text{ and } \lambda_1(Q_{i-2/3}) > 0; \quad (35)$$

$$D1 = F^{(n)}(h, \overline{Q}_{i-2/3}) - F^{(n)}(h, Q_{i-1}), \text{ if } \lambda_1(Q_{i-1}) > 0 \text{ and } \lambda_1(Q_{i-2/3}) \le 0; \quad (36)$$

$$D1 = 0, \text{ if } \lambda_1(Q_{i-1}) \le 0 \text{ and } \lambda_1(Q_{i-2/3}) \le 0; \quad (37)$$

$$D2 = F^{(n)}(h, Q_{i-1/3}) - F^{(n)}(h, Q_{i-2/3}), \text{ if } \lambda_{2,3}(Q_{i-1/3}) > 0; \quad (38)$$

$$D2 = 0, \text{ if } \lambda_{2,3}(Q_{i-1/3}) \le 0; \quad (39)$$

$$D3 = F^{(n)}(h, Q_i) - F^{(n)}(h, Q_{i-1/3}), \text{ if } \lambda_4(Q_{i-1/3}) > 0 \text{ and } \lambda_4(Q_i) > 0; \quad (40)$$

$$D3 = F^{(n)}(h, Q_i) - F^{(n)}(h, \overline{Q}_{i-1/3}), \text{ if } \lambda_4(Q_{i-1/3}) \le 0 \text{ and } \lambda_4(Q_i) > 0; \quad (41)$$

$$D3 = F^{(n)}(h, \overline{Q}_{i-1/3}) - F^{(n)}(h, Q_{i-1/3}), \text{ if } \lambda_4(Q_{i-1/3}) > 0 \text{ and } \lambda_4(Q_i) \le 0; \quad (42)$$

$$D3 = 0, \text{ if } \lambda_4(Q_{i-1/3}) \le 0 \text{ and } \lambda_4(Q_i) \le 0. \quad (43)$$

Chakravarthy and Osher (1983) algorithm. The complete algorithm of Chakravarthy and Osher (1983) to update the dependent variables at the (i,j) cell of the n temporal level to the next n+1 level can be simply write as a concise sequence of steps.

ξ contribution:

1) Evaluate the dependent variables at the intermediate cells between i-1 and i using Eqs. (18) to (22). The metric terms are calculated at i-1/2 interface (pointing to inside the cell);

2) Using Eqs. (23) to (26), evaluate the sonic cells which appear between i-1 and i (if the eigenvalues change signal). The metric terms are calculated at i-1/2 interface (pointing inside the cell);

3) Evaluate the subintegrals D1, D2 and D3 between cells i-1 and i using Eqs. (34) to (43). The fluxes $F^{(n)}$ at the cells of the computational domain and at the intermediate states are evaluated as necessary;

4) Repeat steps 1-3 between cells i and i+1. The metric terms are calculated at the i+1/2 interface (poinitng outside the cell);

5) Substitute the subintegrals and fluxes in Eq. (31) to evaluate the ξ contribution.

η contribution:

6) Repeat steps 1-5 to the cells j-1, j and j+1 and the metric terms calculated at the j-1/2 and j+1/2 interfaces [the formulae to η are obtained substituting areas and volumes at the interfaces (i-1/2,j) and (i+1/2,j) by areas and volumes at interfaces (i,j-1/2) e (i,j+1/2)].

Update:

7) Update the conserved variables using the explicit Euler method to the time march with first order of accuracy:

$$Q_{i,j}^{n+1} = Q_{i,j}^n - \Delta t_{i,j} / V_{i,j} \left[\left(\int_{Q_{i-1,j}}^{Q_{i,j}} \hat{A}^+ dQ + \int_{Q_{i,j}}^{Q_{i+1,j}} \hat{A}^- dQ + \int_{Q_{i,j-1}}^{Q_{i,j}} \hat{B}^+ dQ + \int_{Q_{i,j}}^{Q_{i,j+1}} \hat{B}^- dQ \right) \right], \quad (44)$$

with the terms multiplying $\Delta t_{i,j}$ being evaluated in steps 1-6. This version of the algorithm of flux difference splitting of Chakravarthy and Osher (1983) is first order accurate in space.

3.5 Harten (1983) algorithm

The Harten (1983) dissipation function at the (i+1/2,j) interface is defined by:

$$\{D_{Harten}\}_{i+1/2,j} = [R]_{i+1/2,j} \{-\psi\alpha / \Delta t_{i,j}\}_{i+1/2,j}, \quad (45)$$

with ψ described in Maciel (2008b). The inviscid numerical flux vector to the (i+1/2,j)

interface is described by:

$$F^{(l)}_{i+1/2,j} = \left(E^{(l)}_{\text{int}} h_x + F^{(l)}_{\text{int}} h_y \right) V_{\text{int}} + 0.5 D^{(l)}_{Harten}, \tag{46}$$

3.6 MacCormack (1985) algorithm

Applying Green's theorem to Eq. (1) and adopting a structured mesh notation:

$$\partial Q_{i,j} / \partial t = -1/V \int_{S_{i,j}} (P \cdot n)_{i,j} dS_{i,j} . \tag{47}$$

The time integration is accomplished using the following first order scheme:

$$Q^{n+1}_{i,j} = Q^n_{i,j} - \Delta t / V_{i,j} \int_{S_{i,j}} (P \cdot n)_{i,j} dS_{i,j} , \tag{48}$$

The discretization of the surface integral in Eq. (48) results in:

$$Q^{n+1}_{i,j} = Q^n_{i,j} - \Delta t / V_{i,j} \left[(P \cdot S)_{i,j-1/2} + (P \cdot S)_{i+1/2,j} + (P \cdot S)_{i,j+1/2} + (P \cdot S)_{i-1/2,j} \right]^n . \tag{49}$$

In a generalized curvilinear coordinate system, MacCormack (1984) suggests the use of normalized area vectors, orientated in the positive ξ and η directions. These vectors are defined as:

$$s'_x = s_x / \|S\| \quad \text{and} \quad s'_y = s_y / \|S\| \tag{50}$$

where $\|S\| = \left(s_x^2 + s_y^2 \right)^{0.5}$. The s_x and s_y terms are defined in Maciel (2008b). Equation (49) can be rewritten using the following expressions

$$(P \cdot S)_{i,j-1/2} = -\left(E s'_x + F s'_y \right)_{i,j-1/2} \|S\|_{i,j-1/2} ; \tag{51}$$

$$(P \cdot S)_{i+1/2,j} = \left(E s'_x + F s'_y \right)_{i+1/2,j} \|S\|_{i+1/2,j} ; \tag{52}$$

$$(P \cdot S)_{i,j+1/2} = \left(E s'_x + F s'_y \right)_{i,j+1/2} \|S\|_{i,j+1/2} ; \tag{53}$$

$$(P \cdot S)_{i-1/2,j} = -\left(E s'_x + F s'_y \right)_{i-1/2,j} \|S\|_{i-1/2,j} . \tag{54}$$

Literature commonly references MacCormack schemes as upwind. In reality, it is only the MacCormack scheme (1985) using flux vector splitting, which includes an analysis of propagation of information in characteristic directions, that can be classified as an upwind scheme. The MacCormack scheme (1985) takes into account Steger and Warming's flux vector splitting (1981) and convective fluxes in face (i+1/2,j) are written as:

$$(E)_{i+1/2,j} = A^+_{i+1/2,j} Q_{i,j} + A^-_{i+1/2,j} Q_{i+1,j} \quad \text{and} \quad (F)_{i+1/2,j} = B^+_{i+1/2,j} Q_{i,j} + B^-_{i+1/2,j} Q_{i+1,j} . \tag{55}$$

For example, the convective fluxes are calculated as,

$$(P \cdot S)_{i+1/2,j} = \left[\left(A^+ s'_x + B^+ s'_y \right)_{i+1/2,j} Q_{i,j} + \left(A^- s'_x + B^- s'_y \right)_{i+1/2,j} Q_{i+1,j} \right] \|S\|_{i+1/2,j} ; \tag{56}$$

$$(P \cdot S)_{i,j+1/2} = \left[\left(A^+ s'_x + B^+ s'_y \right)_{i,j+1/2} Q_{i,j} + \left(A^- s'_x + B^- s'_y \right)_{i,j+1/2} Q_{i,j+1} \right] \|S\|_{i,j+1/2} . \tag{57}$$

By definition, the reconstructed Jacobian matrices can be determined as follows:

$$A^{+'}_{i+1/2,j} = A^+_{i+1/2,j} s'_{x_{i+1/2,j}} + B^+_{i+1/2,j} s'_{y_{i+1/2,j}}, \quad A^{-'}_{i+1/2,j} = A^-_{i+1/2,j} s'_{x_{i+1/2,j}} + B^-_{i+1/2,j} s'_{y_{i+1/2,j}} ; \tag{58}$$

$$B_{i,j+1/2}^{+'} = A_{i,j+1/2}^{+} s_{xi,j+1/2}^{'} + B_{i,j+1/2}^{+} s_{yi,j+1/2}^{'} \quad \text{and} \quad B_{i,j+1/2}^{-'} = A_{i,j+1/2}^{-} s_{xi,j+1/2}^{'} + B_{i,j+1/2}^{-} s_{yi,j+1/2}^{'}. \quad (59)$$

The same reasoning is true to other flux faces. In the Steger and Warming's flux vector splitting (1981), it is verified that these positive and negative reconstructed matrices can be determined as:

$$A_{i+1/2,j}^{+'} = T_\xi \Lambda_{i+1/2,j}^{+'} T_\xi^{-1}, \quad A_{i+1/2,j}^{-'} = T_\xi \Lambda_{i+1/2,j}^{'} T_\xi^{-1} - A_{i+1/2,j}^{+'}, \quad B_{i,j+1/2}^{+'} = T_\eta \Lambda_{i,j+1/2}^{+'} T_\eta^{-1}; \quad (60)$$

$$B_{i,j+1/2}^{-'} = T_\eta \Lambda_{i,j+1/2}^{'} T_\eta^{-1} - B_{i,j+1/2}^{+'}, \quad (61)$$

where matrices $T_\xi, T_\xi^{-1}, T_\eta$ and T_η^{-1} are defined in subsection 4.2. In this case, based on the equivalence between finite difference and finite volume formulations, in generalized curvilinear coordinates, it is possible to obtain for the predictor step:

- Matrices $A_{i+1/2,j}^{+'}$ and $A_{i+1/2,j}^{-'}$:

$$(T_\xi \text{ and } T_\xi^{-1}) \rightarrow k_x = s_{xi+1/2,j}^{'}, k_y = s_{yi+1/2,j}^{'}, \tilde{k}_x = s_{xi+1/2,j}^{'} \text{ and } \tilde{k}_y = s_{yi+1/2,j}^{'}, \text{ where } k_x, \ k_y,$$

$\tilde{k}_x$ and $\tilde{k}_y$ are parameters to construct matrices T_ξ and T_ξ^{-1}, similars to $h_x^{'}$ and $h_y^{'}$. Eigenvalues of Euler equations in ξ direction are defined by:

$$\lambda_1^{'} = s_{xi+1/2,j}^{'} u + s_{yi+1/2,j}^{'} v, \quad \lambda_2^{'} = s_{xi+1/2,j}^{'} u + s_{yi+1/2,j}^{'} v, \quad \lambda_3^{'} = s_{xi+1/2,j}^{'} u + s_{yi+1/2,j}^{'} v + a; \quad (62)$$

$$\lambda_4^{'} = s_{xi+1/2,j}^{'} u + s_{yi+1/2,j}^{'} v - a. \quad (63)$$

- Matrices $B_{i,j+1/2}^{+'}$ and $B_{i,j+1/2}^{-'}$:

$$(T_\eta \text{ and } T_\eta^{-1}) \rightarrow k_x = s_{xi,j+1/2}^{'}, k_y = s_{yi,j+1/2}^{'}, \tilde{k}_x = s_{xi,j+1/2}^{'} \text{ and } \tilde{k}_y = s_{yi,j+1/2}^{'}, \text{ where } k_x, \ k_y,$$

$\tilde{k}_x$ and $\tilde{k}_y$ are parameters to construct matrices T_η and T_η^{-1}, similars to $h_x^{'}$ and $h_y^{'}$. Eigenvalues of Euler equations in η direction are:

$$\lambda_1^{'} = s_{xi,j+1/2}^{'} u + s_{yi,j+1/2}^{'} v, \quad \lambda_2^{'} = s_{xi,j+1/2}^{'} u + s_{yi,j+1/2}^{'} v, \quad \lambda_3^{'} = s_{xi,j+1/2}^{'} u + s_{yi,j+1/2}^{'} v + a; \quad (64)$$

$$\lambda_4^{'} = s_{xi,j+1/2}^{'} u + s_{yi,j+1/2}^{'} v - a. \quad (65)$$

Calculating the convective flux terms of Eq. (49), according to Eqs. (51) through (61), and determining the reconstructed Jacobian matrices like (62) and (63) and (64) and (65), the MacCormack scheme (1985), in its explicit version, is written as:

- Predictor step:

$$\Delta Q_{i,j}^n = -\Delta t / V_{i,j} \Big[(B_{i,j}^{+'} Q_{i,j-1} + B_{i,j}^{-'} Q_{i,j}) \big\| S_{i,j-1/2} \big\| + (A_{i+1,j}^{+'} Q_{i,j} + A_{i+1,j}^{-'} Q_{i+1,j}) \big\| S_{i+1/2,j} \big\| +$$

$$(B_{i,j+1}^{+'} Q_{i,j} + B_{i,j+1}^{-'} Q_{i,j+1}) \big\| S_{i,j+1/2} \big\| + (A_{i,j}^{+'} Q_{i-1,j} + A_{i,j}^{-'} Q_{i,j}) \big\| S_{i-1/2,j} \big\| \Big]^n \quad ; \quad (66)$$

$$Q_{p_{i,j}}^{n+1} = Q_{i,j}^n + \Delta Q_{i,j}^n$$

- Corrector step:

$$\Delta Q_{c_{i,j}}^{n+1} = -\Delta t / V_{i,j} \left[(B_{i,j-1}^{+} Q_{i,j-1} + B_{i,j-1}^{-} Q_{i,j})_p \left\| S_{i,j-1/2} \right\| + (A_{i,j}^{+} Q_{i,j} + A_{i,j}^{-} Q_{i+1,j})_p \left\| S_{i+1/2,j} \right\| \right.$$

$$\left. + (B_{i,j}^{+} Q_{i,j} + B_{i,j}^{-} Q_{i,j+1})_p \left\| S_{i,j+1/2} \right\| + (A_{i-1,j}^{+} Q_{i-1,j} + A_{i-1,j}^{-} Q_{i,j})_p \left\| S_{i-1/2,j} \right\| \right]^{n+1} . \quad (67)$$

$$Q_{i,j}^{n+1} = \frac{1}{2} \left(Q_{i,j}^{n} + Q_{p_{i,j}}^{n+1} + \Delta Q_{c_{i,j}}^{n+1} \right)$$

3.7 Frink, Parikh and Pirzadeh (1991) algorithm

The Frink, Parikh and Pirzadeh (1991) dissipation function can be written in terms of three flux components, each one associated with a distinct eigenvalue of the Euler equations:

$$D_{FPP} = \left| \Delta \widetilde{F}_1 \right| + \left| \Delta \widetilde{F}_3 \right| + \left| \Delta \widetilde{F}_4 \right|, \quad (68)$$

where:

$$\left| \Delta \widetilde{F}_1 \right| = \left| \widetilde{\psi}_1 \right| \left\{ \left(\Delta \rho - \frac{\Delta p}{\widetilde{a}^2} \right) \begin{bmatrix} 1 \\ \widetilde{u} \\ \widetilde{v} \\ \dfrac{\widetilde{u}^2 + \widetilde{v}^2}{2} \end{bmatrix} + \widetilde{\rho} \begin{bmatrix} 0 \\ \Delta u - n_x \Delta U \\ \Delta v - n_y \Delta U \\ \widetilde{u} \Delta u + \widetilde{v} \Delta v - \widetilde{U} \Delta U \end{bmatrix} \right\}; \quad (69)$$

$$\left| \Delta \widetilde{F}_{3,4} \right| = \left| \widetilde{\psi}_{3,4} \right| \left(\frac{\Delta p \pm \widetilde{\rho} \widetilde{a} \Delta U}{2\widetilde{a}^2} \right) \begin{bmatrix} 1 \\ \widetilde{u} \pm n_x \widetilde{a} \\ \widetilde{v} \pm n_y \widetilde{a} \\ \widetilde{H} \pm \widetilde{U} \widetilde{a} \end{bmatrix}, \quad (70)$$

with $\widetilde{U} = \widetilde{u} n_x + \widetilde{v} n_y$; $\Delta U = n_x \Delta u + n_y \Delta v$; $\widetilde{\rho}$, $\widetilde{H}$, $\widetilde{u}$ and $\widetilde{v}$ are obtained from Roe (1981) average; $\widetilde{a}$ is the speed of sound obtained from the average variables; and $\Delta(\cdot) = (\cdot)_{i+1,j} - (\cdot)_{i,j}$, to the (i+1/2,j) interface.

The present author suggests the implementation of an entropy function $\widetilde{\psi}$ aiming to avoid zero contributions from the system's eigenvalues to the dissipation function of Frink, Parikh and Pirzadeh (1991). The entropy condition is implemented in the eigenvalues $\widetilde{\lambda}_1 = \widetilde{U}$, $\widetilde{\lambda}_3 = \widetilde{U} + \widetilde{a}$ and $\widetilde{\lambda}_4 = \widetilde{U} - \widetilde{a}$ of the following way:

$$\widetilde{\psi}_l = \begin{cases} |Z_l|, & \text{if } |Z_l| \geq \varepsilon \\ 0.5 \left(Z_l^2 + \varepsilon^2 \right) / \varepsilon, & \text{if } |Z_l| < \varepsilon \end{cases}, \quad \text{with: } Z_l = \widetilde{\lambda}_l, \quad (71)$$

where the ε parameter assumes the value 0.01, recommended by the present author. The convective numerical flux vector at the (i+1/2,j) interface is defined as:

$$F_{i+1/2,j}^{(l)} = \left(E_{\text{int}}^{(l)} n_{x_{i+1/2,j}} + F_{\text{int}}^{(l)} n_{y_{i+1/2,j}} - 0.5 D_{FPP}^{(l)} \right) S \Big|_{i+1/2,j}, \quad (72)$$

with S, n_x and n_y calculated as the same way as indicated in Maciel (2008b).

3.8 Liou and Steffen Jr. (1993) algorithm

The definition of the residual or the numerical flux vector of the Liou and Steffen Jr. (1993) scheme is defined by Eq. (10). The definition of the ϕ dissipation term which determines the Liou and Steffen Jr. (1993) scheme, based on Radespiel and Kroll (1995), is:

$$\phi_{i+1/2,j} = \phi_{i+1/2,j}^{LS} = \left| M_{i+1/2,j} \right|. \tag{73}$$

3.9 Radespiel and Kroll (1995) algorithm

The definition of the residual or the numerical flux vector at the (i+1/2,j) interface of the Radespiel and Kroll (1995) scheme is defined by Eq. (10). The definition of the ϕ dissipation term which determines the Radespiel and Kroll (1995) scheme combines the Van Leer (1982) scheme and the Liou and Steffen Jr. (1993) (AUSM) scheme. Hence,

$$\phi_{i+1/2,j} = (1-\omega)\phi_{i+1/2,j}^{VL} + \omega\phi_{i+1/2,j}^{LS}, \tag{74}$$

with:

$$\phi_{i+1/2,j}^{VL} = \begin{cases} \left| M_{i+1/2,j} \right|, & if \left| M_{i+1/2,j} \right| \geq 1; \\ \left| M_{i+1/2,j} \right| + \frac{1}{2}(M_R - 1)^2, & if \ 0 \leq M_{i+1/2,j} < 1; \\ \left| M_{i+1/2,j} \right| + \frac{1}{2}(M_L + 1)^2, & if \ -1 < M_{i+1/2,j} \leq 0; \end{cases} \quad and \quad \phi_{i+1/2,j}^{LS} = \begin{cases} \left| M_{i+1/2,j} \right|, & if \left| M_{i+1/2,j} \right| > \tilde{\delta} \\ \dfrac{(M_{i+1/2,j})^2 + \tilde{\delta}^2}{2\tilde{\delta}}, & if \left| M_{i+1/2,j} \right| \leq \tilde{\delta} \end{cases}, \tag{75}$$

where $\tilde{\delta}$ is a small parameter, $0 < \tilde{\delta} \leq 0.5$, and ω is a constant, $0 \leq \omega \leq 1$. In this work, the values used to $\tilde{\delta}$ and ω were: 0.2 and 0.5, respectively.

4 IMPLICIT FORMULATIONS

Except the implicit MacCormack (1985) first order scheme, all other implicit schemes studied in this work used an ADI formulation to solve the algebraic nonlinear system of equations. In these cases, the nonlinear system of equations is linearized considering the implicit operator evaluated at the time "*n*" and, posteriorly, the five-diagonal system of linear algebraic equations is factored in two three-diagonal systems of linear algebraic equations, each one associated with a particular spatial direction. Thomas algorithm is employed to solve these two three-diagonal systems. All the implicit schemes studied in this work were only applicable to the solution of the Euler equations, which implies that only the convective contributions were considered in the RHS ("Right Hand Side") operator.

4.1 Implicit formulation to the Roe (1981), the Chakravarthy and Osher (1983), the Harten (1983) and the Frink, Parikh and Pirzadeh (1991) first order algorithms

The ADI form to the Roe (1981), the Chakravarthy and Osher (1983), the Harten (1983) and the Frink, Parikh and the Pirzadeh (1991) first order schemes is defined by the following two step algorithm:

$$\left\{ I + \Delta t_{i,j} \Delta_\xi^- K_{i+1/2,j}^+ + \Delta t_{i,j} \Delta_\xi^+ K_{i+1/2,j}^- \right\} \Delta Q_{i,j}^* = \left[RHS_{(FDS)} \right]_{i,j}^n, \text{ to the } \xi \text{ direction;} \tag{76}$$

$$\left\{ I + \Delta t_{i,j} \Delta_\eta^- J_{i,j+1/2}^+ + \Delta t_{i,j} \Delta_\eta^+ J_{i,j+1/2}^- \right\} \Delta Q_{i,j}^{n+1} = \Delta Q_{i,j}^*, \text{ to the } \eta \text{ direction;} \tag{77}$$

$$Q_{i,j}^{n+1} = Q_{i,j}^n + \Delta Q_{i,j}^{n+1}, \tag{78}$$

where:

$$K_{i\pm1/2,j}^{\pm} = [R]_{i\pm1/2,j}^{n} \Omega_{i\pm1/2,j}^{\pm} [R^{-1}]_{i\pm1/2,j}^{n}; \quad J_{i,j\pm1/2}^{\pm} = [R]_{i,j\pm1/2}^{n} \Phi_{i,j\pm1/2}^{\pm} [R^{-1}]_{i,j\pm1/2}^{n}; \tag{79}$$

$$\Omega_{i\pm1/2,j}^{\pm} = diag\left[(\lambda_{\xi}^{l})^{\pm}\right]_{i\pm1/2,j}^{n}; \quad \Phi_{i,j\pm1/2}^{\pm} = diag\left[(\lambda_{\eta}^{l})^{\pm}\right]_{i,j\pm1/2}^{n}; \tag{80}$$

$$(\lambda_{\xi}^{l})^{\pm} = 0.5(\lambda_{\xi}^{l} \pm |\lambda_{\xi}^{l}|), \ (\lambda_{\eta}^{l})^{\pm} = 0.5(\lambda_{\eta}^{l} \pm |\lambda_{\eta}^{l}|), \ \Delta_{\xi}^{-} = (\cdot)_{i,j} - (\cdot)_{i-1,j}, \ \Delta_{\xi}^{+} = (\cdot)_{i+1,j} - (\cdot)_{i,j}; \tag{81}$$

$$\Delta_{\eta}^{-} = (\cdot)_{i,j} - (\cdot)_{i,j-1}, \ \Delta_{\eta}^{+} = (\cdot)_{i,j+1} - (\cdot)_{i,j}. \tag{82}$$

In Equation (79), the R matrix is defined in Maciel (2008a,b); $diag[\cdot]$ is a diagonal matrix; in Eqs. (80) and (81), "l" assumes values from 1 to 4 and λ's are the eigenvalues of the Euler equations, defined in Maciel (2008a,b). The matrix R^{-1} is defined as:

$$R^{-1} = \begin{bmatrix} \frac{1}{2}\left[\frac{\gamma-1}{a_{int}^2}\frac{(u_{int}^2+v_{int}^2)}{2}+\frac{1}{a_{int}}\left(u_{int}h_x^{'}+v_{int}h_y^{'}\right)\right] & \frac{1}{2}\left(-\frac{\gamma-1}{a_{int}^2}u_{int}-\frac{h_x^{'}}{a_{int}}\right) & \frac{1}{2}\left(-\frac{\gamma-1}{a_{int}^2}v_{int}-\frac{h_y^{'}}{a_{int}}\right) & \frac{\gamma-1}{2a_{int}^2} \\ 1-\frac{\gamma-1}{a_{int}^2}\frac{(u_{int}^2+v_{int}^2)}{2} & \frac{\gamma-1}{a_{int}^2}u_{int} & \frac{\gamma-1}{a_{int}^2}v_{int} & -\frac{\gamma-1}{a_{int}^2} \\ -\left(h_x^{'}v_{int}-h_y^{'}u_{int}\right) & -h_y^{'} & h_x^{'} & 0 \\ \frac{1}{2}\left[\frac{\gamma-1}{a_{int}^2}\frac{(u_{int}^2+v_{int}^2)}{2}-\frac{1}{a_{int}}\left(u_{int}h_x^{'}+v_{int}h_y^{'}\right)\right] & \frac{1}{2}\left(-\frac{\gamma-1}{a_{int}^2}u_{int}+\frac{h_x^{'}}{a_{int}}\right) & \frac{1}{2}\left(-\frac{\gamma-1}{a_{int}^2}v_{int}+\frac{h_y^{'}}{a_{int}}\right) & \frac{\gamma-1}{2a_{int}^2} \end{bmatrix}, \tag{83}$$

with $h_x^{'}$ and $h_y^{'}$ defined according to Maciel (2008a,b); u_{int} and v_{int} are the Cartesian components of velocity at the cell interface; a_{int} is the speed of sound at the cell interface; and γ is the ratio of specific heats. The interface properties are defined either by arithmetical average or by Roe (1981) average. In this work, the Roe (1981) average was used. The $RHS_{(FDS)}$ is defined as the residual of the flux difference splitting schemes, which is defined, for instance, by the Roe (1981) scheme as:

$$\left[RHS_{(Roe)}\right]_{i,j}^{n} = -\Delta t_{i,j}/V_{i,j}\left(F_{i+1/2,j}^{(Roe)} - F_{i-1/2,j}^{(Roe)} + F_{i,j+1/2}^{(Roe)} - F_{i,j-1/2}^{(Roe)}\right)^{n}, \tag{84}$$

with $F_{i+1/2,j}^{(Roe)}$ defined in Maciel (2008a, 2011b); $V_{i,j}$ is the cell volume; and $\Delta t_{i,j}$ is the time step. The other schemes follow similar formulae. Details of the RHS definition to the flux difference splitting schemes see Maciel (2008a,b and 2011b). This implementation is first order accurate in time due to the definition of Ω and of Φ, as reported in Yee, Warming and Harten (1985), and is first order accurate in space due to the RHS of the numerical schemes.

4.2 Implicit formulation to the Steger and Warming (1981), the Van Leer (1982), the Liou and Steffen Jr. (1993) and the Radespiel and Kroll (1995) first order algorithms

The ADI form to the Steger and Warming (1981), the Van Leer (1982), the Liou and Steffen Jr. (1993) and the Radespiel and Kroll (1995) first order schemes is defined by the following two step algorithm:

$$\left\{I + \Delta t_{i,j}\Delta_{\xi}^{-}A_{i+1/2,j}^{+} + \Delta t_{i,j}\Delta_{\xi}^{+}A_{i+1/2,j}^{-}\right\}\Delta Q_{i,j}^{*} = \left[RHS_{(FVS)}\right]_{i,j}^{n}, \text{ to the } \xi \text{ direction}; \tag{85}$$

$$\left\{I + \Delta t_{i,j}\Delta_\eta^- B_{i,j+1/2}^+ + \Delta t_{i,j}\Delta_\eta^+ B_{i,j+1/2}^-\right\}\Delta Q_{i,j}^{n+1} = \Delta Q_{i,j}^*, \text{ to the } \eta \text{ direction;} \tag{86}$$

$$Q_{i,j}^{n+1} = Q_{i,j}^n + \Delta Q_{i,j}^{n+1}, \tag{87}$$

where the matrices $A^\pm$ and $B^\pm$ are defined as:

$$A_{i\pm1/2,j}^\pm = [T]_{i\pm1/2,j}^n \Omega_{i\pm1/2,j}^\pm [T^{-1}]_{i\pm1/2,j}^n; \quad B_{i,j\pm1/2}^\pm = [T]_{i,j\pm1/2}^n \Phi_{i,j\pm1/2}^\pm [T^{-1}]_{i,j\pm1/2}^n; \tag{88}$$

$$\Omega_{i\pm1/2,j}^\pm = diag\left[\left(\lambda_\xi^l\right)^\pm\right]_{i\pm1/2,j}^n; \quad \Phi_{i,j\pm1/2}^\pm = diag\left[\left(\lambda_\eta^l\right)^\pm\right]_{i,j\pm1/2}^n; \tag{89}$$

with the similarity transformation matrices defined by:

$$T = \begin{bmatrix} 1 & 0 & \alpha & \alpha \\ u_{int} & h_y'\rho_{int} & \alpha(u_{int} + h_x'a_{int}) & \alpha(u_{int} - h_x'a_{int}) \\ v_{int} & -h_x'\rho_{int} & \alpha(v_{int} + h_y'a_{int}) & \alpha(v_{int} - h_y'a_{int}) \\ \dfrac{\phi^2}{\gamma-1} & \rho_{int}(h_y'u_{int} - h_x'v_{int}) & \alpha\left(\dfrac{\phi^2 + a_{int}^2}{\gamma-1} + a_{int}\tilde\theta\right) & \alpha\left(\dfrac{\phi^2 + a_{int}^2}{\gamma-1} - a_{int}\tilde\theta\right) \end{bmatrix}; \tag{90}$$

$$\alpha = \rho_{int}/\left(\sqrt{2}a_{int}\right), \ \beta = 1/\left(\sqrt{2}\rho_{int}a_{int}\right), \ \phi^2 = (\gamma-1)\frac{u_{int}^2 + v_{int}^2}{2}, \ \tilde\theta = h_x'u_{int} + h_y'v_{int}; \tag{91}$$

$$T^{-1} = \begin{bmatrix} 1 - \dfrac{\phi^2}{a_{int}^2} & (\gamma-1)\dfrac{u_{int}}{a_{int}^2} & (\gamma-1)\dfrac{v_{int}}{a_{int}^2} & -\dfrac{\gamma-1}{a_{int}^2} \\ -\dfrac{h_y'u_{int} - h_x'v_{int}}{\rho_{int}} & \dfrac{h_y'}{\rho_{int}} & -\dfrac{h_x'}{\rho_{int}} & 0 \\ \beta(\phi^2 - a_{int}\tilde\theta) & \beta[h_x'a_{int} - (\gamma-1)u_{int}] & \beta[h_y'a_{int} - (\gamma-1)v_{int}] & \beta(\gamma-1) \\ \beta(\phi^2 + a_{int}\tilde\theta) & -\beta[h_x'a_{int} + (\gamma-1)u_{int}] & -\beta[h_y'a_{int} + (\gamma-1)v_{int}] & \beta(\gamma-1) \end{bmatrix}, \tag{92}$$

with ρ_{int} defined as the interface density. The properties defined at interface are calculated by arithmetical average. The *RHS(FVS)* is defined as the residual of the flux vector splitting schemes, similar to Eq. (84). Details of the *RHS* definition to the flux vector splitting schemes see Maciel (2008a,b and 2011b). This implementation is first order accurate in time.

4.3 Implicit formulation to the MacCormack (1985) first order algorithm

The MacCormack implicit scheme (1985) uses the development described in subsection 3.6 with flux vector splitting to obtain a pentadiagonal full block linear system. This system presents a dominant main diagonal in comparison to the other diagonals. With this procedure, when large time steps are considered, the resulting algorithm is closer to the Newton method and an excellent convergence rate to the steady state solution is reached.

It is noted that the pentadiagonal system described by Eqs. (93) and (94) has a dominant main diagonal when compared to the adjacent diagonals (MacCormack, 1984, and MacCormack, 1985). This is the main advantage of MacCormack's implicit scheme (1985). One disadvantage is that, with this implementation, MacCormack method (1985) becomes a first order scheme in space.

This five-diagonal system, in the predictor and corrector steps, typical of MacCormack's schemes, is solved by a symmetric line Gauss-Seidel relaxation method with two sweeps: one forward and other backward. This procedure results in a tridiagonal linear system in the η direction. The first time step adopts the trivial solution for the correction in the conserved

variables when solving the predictor step. In the corrector step the currently available solution for correction is used. Afterwards, all other Gauss-Seidel sweeps use the latest available values for the corrections. According to MacCormack (1984), the symmetric line Gauss-Seidel relaxation method should be solved only with two sweeps to avoid excessive computational cost.

- Predictor step:

$$\Delta Q_{i,j}^n = -\Delta t/V_{i,j}\left[(B_{i,j}^{+}Q_{i,j-1} + B_{i,j}^{-}Q_{i,j})\left\|S_{i,j-1/2}\right\| + (A_{i+1,j}^{+}Q_{i,j} + A_{i+1,j}^{-}Q_{i+1,j})\left\|S_{i+1/2,j}\right\|\right.$$

$$\left. + (B_{i,j+1}^{+}Q_{i,j} + B_{i,j+1}^{-}Q_{i,j+1})\left\|S_{i,j+1/2}\right\| + (A_{i,j}^{+}Q_{i-1,j} + A_{i,j}^{-}Q_{i,j})\left\|S_{i-1/2,j}\right\|\right]^n$$

$$\left(-\Delta t/V_{i,j}\ B_{i,j}^{+}\left\|S_{i,j-1/2}\right\|\right)^n \delta Q_{p_{i,j-1}}^{n+1} + \left\{I + \Delta t/V_{i,j}\left[-B_{i,j}^{-}\left\|S_{i,j-1/2}\right\| + A_{i+1,j}^{+}\left\|S_{i+1/2,j}\right\| + B_{i,j+1}^{+}\left\|S_{i,j+1/2}\right\| - A_{i,j}^{-}\left\|S_{i-1/2,j}\right\|\right]\right\}^n \delta Q_{p_{i,j}}^{n+1} ;$$

$$+ \left(\Delta t/V_{i,j}\ B_{i,j+1}^{-}\left\|S_{i,j+1/2}\right\|\right)^n \delta Q_{p_{i,j+1}}^{n+1} + \left(-\Delta t/V_{i,j}\ A_{i,j}^{+}\left\|S_{i-1/2,j}\right\|\right)^n \delta Q_{p_{i-1,j}}^{n+1} + \left(\Delta t/V_{i,j}\ A_{i+1,j}^{-}\left\|S_{i+1/2,j}\right\|\right)^n \delta Q_{p_{i+1,j}}^{n+1} = \Delta Q_{i,j}^n$$

$$Q_{p_{i,j}}^{n+1} = Q_{i,j}^n + \delta Q_{p_{i,j}}^{n+1}$$

(93)

- Corrector step:

$$\Delta Q_{i,j}^{n+1} = -\Delta t/V_{i,j}\left[(B_{i,j-1}^{+}Q_{i,j-1} + B_{i,j-1}^{-}Q_{i,j})_p\left\|S_{i,j-1/2}\right\| + (A_{i,j}^{+}Q_{i,j} + A_{i,j}^{-}Q_{i+1,j})_p\left\|S_{i+1/2,j}\right\| + \right.$$

$$\left. (B_{i,j}^{+}Q_{i,j} + B_{i,j}^{-}Q_{i,j+1})_p\left\|S_{i,j+1/2}\right\| + (A_{i-1,j}^{+}Q_{i-1,j} + A_{i-1,j}^{-}Q_{i,j})_p\left\|S_{i-1/2,j}\right\|\right]^{n+1}$$

$$\left(-\Delta t/V_{i,j}\ B_{i,j-1}^{+}\left\|S_{i,j-1/2}\right\|\right)_p^{n+1} \delta Q_{i,j-1}^{n+1} + \left\{I + \Delta t/V_{i,j}\left[-B_{i,j-1}^{-}\left\|S_{i,j-1/2}\right\| + A_{i,j}^{+}\left\|S_{i+1/2,j}\right\| + B_{i,j}^{+}\left\|S_{i,j+1/2}\right\| - A_{i-1,j}^{-}\left\|S_{i-1/2,j}\right\|\right]\right\}_p^{n+1} \delta Q_{i,j}^{n+1} .$$

$$+ \left(\Delta t/V_{i,j}\ B_{i,j}^{-}\left\|S_{i,j+1/2}\right\|\right)_p^{n+1} \delta Q_{i,j+1}^{n+1} + \left(-\Delta t/V_{i,j}\ A_{i-1,j}^{+}\left\|S_{i-1/2,j}\right\|\right)_p^{n+1} \delta Q_{i-1,j}^{n+1} + \left(\Delta t/V_{i,j}\ A_{i,j}^{-}\left\|S_{i+1/2,j}\right\|\right)_p^{n+1} \delta Q_{i+1,j}^{n+1} = \Delta Q_{i,j}^{n+1}$$

$$Q_{i,j}^{n+1} = \frac{1}{2}\left(Q_{i,j}^n + Q_{p_{i,j}}^{n+1} + \delta Q_{i,j}^{n+1}\right)$$

(94)

MacCormack's implicit scheme (1985) is obtained using the backward Euler method to accomplish time integration in both predictor and corrector steps, resulting in the above scheme.

5 SPATIALLY VARIABLE TIME STEP

The basic idea of this procedure consists in keeping constant the CFL number in all calculation domain, allowing, hence, the use of appropriated time steps to each specific mesh region during the convergence process. Hence, according to the definition of the CFL number, it is possible to write:

$$\Delta t_{i,j} = CFL(\Delta s)_{i,j}/c_{i,j} ,$$

(95)

where CFL is the "Courant-Friedrichs-Lewy" number to provide numerical stability to the

scheme; $c_{i,j} = \left[\left(u^2 + v^2\right)^{0.5} + a\right]_{i,j}$ is the maximum characteristic speed of information propagation in the calculation domain; and $\left(\Delta s\right)_{i,j}$ is a characteristic length of information transport. On a finite volume context, $\left(\Delta s\right)_{i,j}$ is chosen as the minor value found between the minor centroid distance, involving the (i,j) cell and a neighbor, and the minor cell side length.

6 RESULTS

Tests were performed in a microcomputer with processor INTEL CELERON, 1.5GHz of clock, and 1.0Gbytes of RAM. Converged results occurred to 4 orders of reduction in the maximum residual value. An entrance angle equal to 0.0° and a freestream Mach number of 3.0 were employed as initial conditions. The ratio of specific heats, γ, assumed the value 1.4. The initial and boundary conditions to this supersonic flow are described in Jameson and Mavriplis (1986) and in Maciel (2002, 2011b).

6.1 Compression corner physical problem – Explicit simulations

The compression corner configuration is described in Fig. 2. The corner inclination angle is 10°. An algebraic mesh of 70x50 points or composed of 3,381 rectangular cells and 3,500 nodes was used and is shown in Fig. 3. The points are equally spaced in both directions.
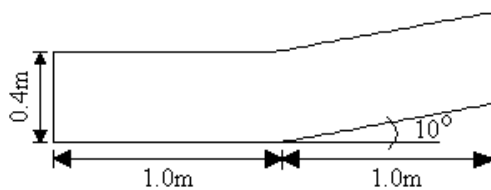
Figure 2: Compression Corner Configuration.
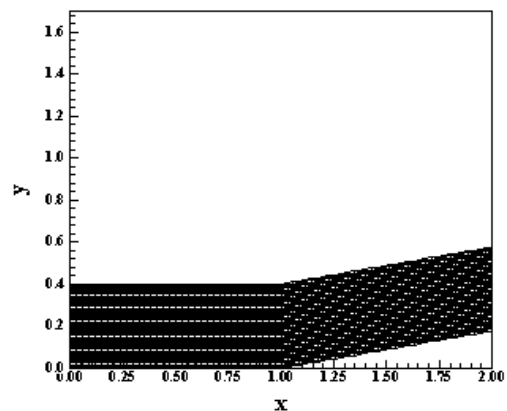
Figure 3: Compression Corner Mesh.

Figures 4 to 12 exhibit the pressure contours obtained by the Roe (1981), the Steger and Warming (1981), the Van Leer (1982), the Chakravarthy and Osher (1983), the Harten (1983), the MacCormack (1985), the Frink, Parikh and Pirzadeh (1991), the Liou and Steffen Jr. (1993) and the Radespiel and Kroll (1995) first order schemes, respectively, to the explicit case. As can be observed the most severe pressure after the shock is captured by the Liou and Steffen Jr. (1993) first order scheme. The smallest shock wave thickness is also captured by the Liou and Steffen Jr. (1993) first order scheme. All solutions present the shock wave smeared out due to the predominant diffusive characteristics of first order schemes. To a comparison involving the shock wave thickness obtained by first order schemes with that generated by second order TVD schemes, see the works of Maciel (2010 and 2011a,c).

Figure 13 shows the wall pressure distributions generated by all the studied schemes in this work, to the explicit case. They are compared with the oblique shock wave theory. All solutions present a smooth behavior typical of first order schemes, except the Liou and Steffen Jr. (1993) first order scheme, which present a peak at the beginning of the compression corner. Even so, all solutions capture the shock discontinuity using three cells.
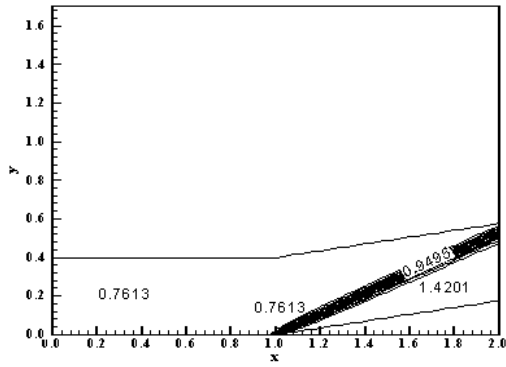
Figure 4: Pressure Contours (Roe).
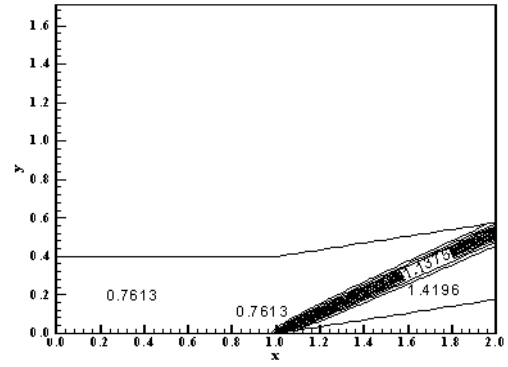
Figure 5: Pressure Contours (SW).
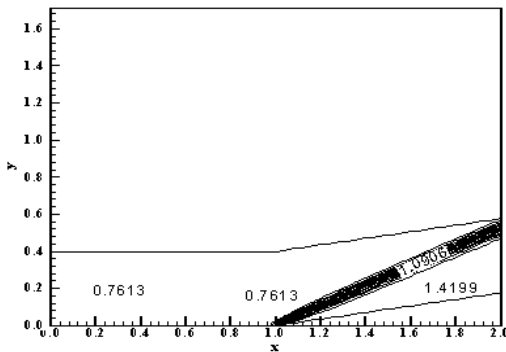
Figure 6: Pressure Contours (VL).
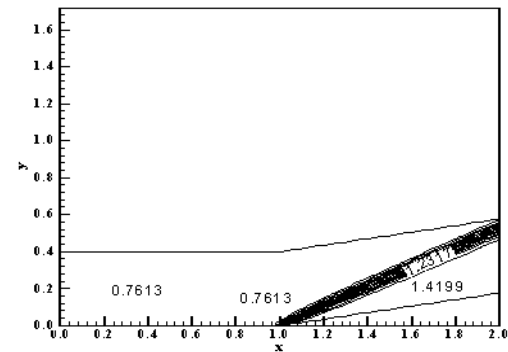
Figure 7: Pressure Contours (CO).
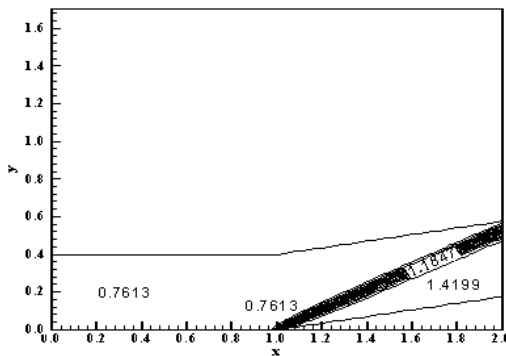
Figure 8: Pressure Contours (Harten).
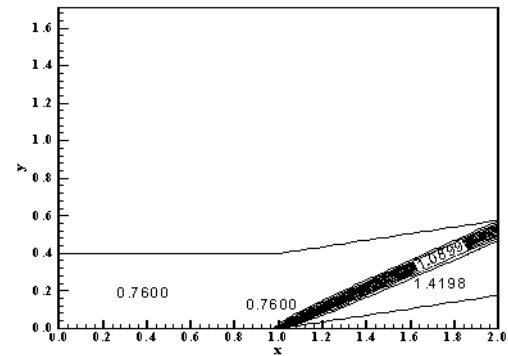
Figure 9: Pressure Contours (Mac).
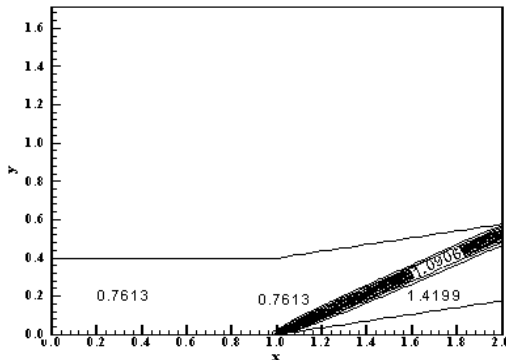
Figure 10: Pressure Contours (FPP).
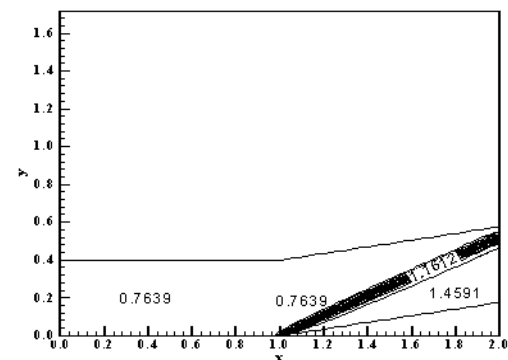
Figure 11: Pressure Contours (LS).
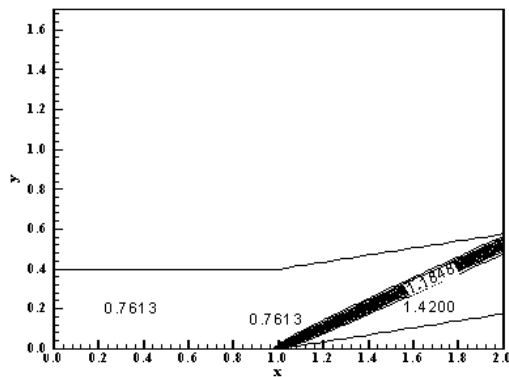
Figure 12: Pressure Contours (RK).
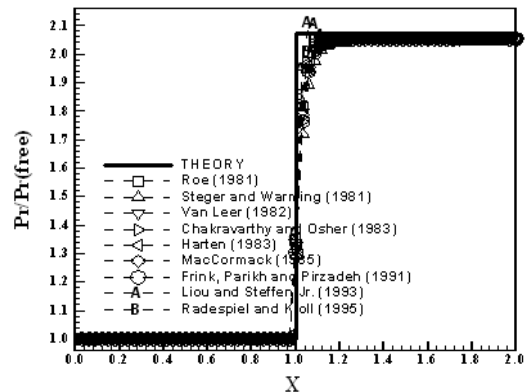
Figure 13: Wall Pressure Distributions (Exp).

All solutions slightly underpredict the shock plateau. The best wall pressure distribution obtained in this explicit case is due to the Radespiel and Kroll (1995) first order algorithm.

One way to quantitatively verify if the solutions generated by each scheme are satisfactory consists in determining the shock angle of the oblique shock wave, β, measured in relation to the initial direction of the flow field. Anderson Jr. (1984) (pages 352 and 353) presents a diagram with values of the shock angle, β, to oblique shock waves. The value of this angle is determined as function of the freestream Mach number and of the deflection angle of the flow after the shock wave, ϕ. To the compression corner problem, ϕ = 10º (corner inclination angle) and the freestream Mach number is 3.0, resulting from this diagram a value to β equals to 27.5º. Using a transfer in Figures 4 to 12, it is possible to obtain the values of β to each scheme, as well the respective errors, shown in Tab. 1. As can be observed, the Harten (1983) first order scheme has yielded the best result. Errors less than 5.00% were observed.

Algorithm:	β (°):	Error (%):
Roe (1981)	28.2	2.55
Steger and Warming (1981)	28.5	3.64
Van Leer (1982)	28.3	2.91
Chakravarthy and Osher (1983)	28.5	3.64
Harten (1983)	27.9	1.45
MacCormack (1985)	28.8	4.73
Frink, Parikh and Pirzadeh (1991)	28.4	3.27
Liou and Steffen Jr. (1993)	28.0	1.82
Radespiel and Kroll (1995)	28.4	3.27

Table 1: Shock angle and percentage errors to the compression corner problem (Explicit case).

6.2 Compression corner physical problem – Implicit simulations

Figures 14 to 22 exhibit the pressure contours obtained by the Roe (1981), the Steger and Warming (1981), the Van Leer (1982), the Chakravarthy and Osher (1983), the Harten (1983), the MacCormack (1985), the Frink, Parikh and Pirzadeh (1991), the Liou and Steffen Jr. (1993) and the Radespiel and Kroll (1995) first order schemes, respectively, to the implicit case. As can be observed the most severe pressure after the shock is again captured by the Liou and Steffen Jr. (1993) first order scheme. The smallest shock wave thickness is also captured by the Liou and Steffen Jr. (1993) first order scheme. All solutions present the shock

wave smeared out due to the predominant diffusive characteristics of first order schemes.
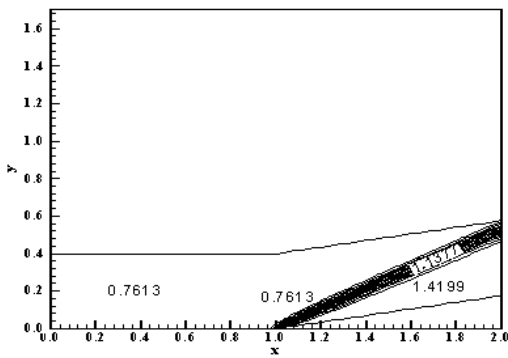
Figure 14: Pressure Contours (Roe).
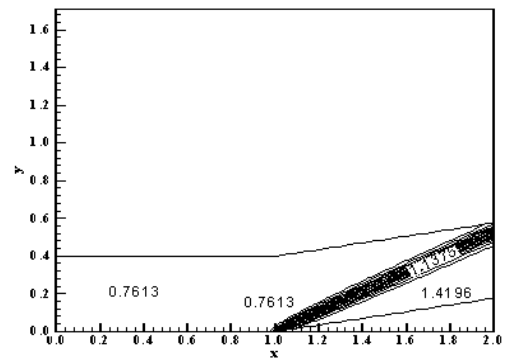
Figure 15: Pressure Contours (SW).
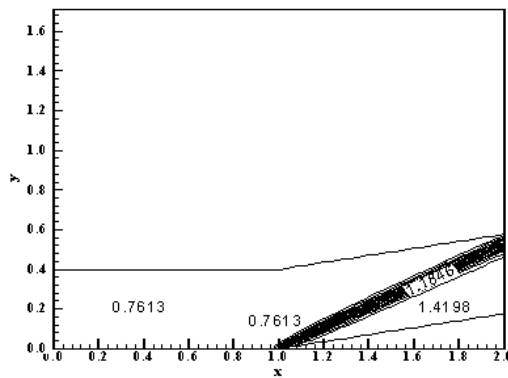
Figure 16: Pressure Contours (VL).
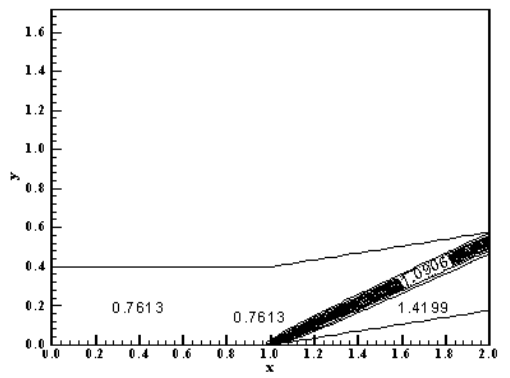
Figure 17: Pressure Contours (CO).
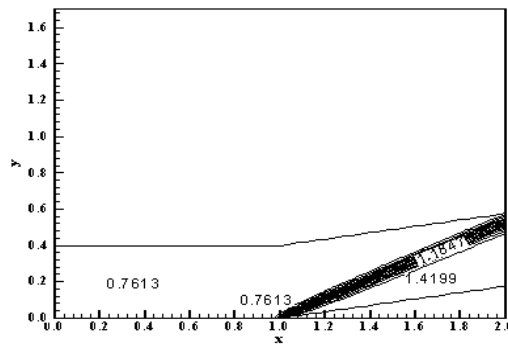
Figure 18: Pressure Contours (Harten).
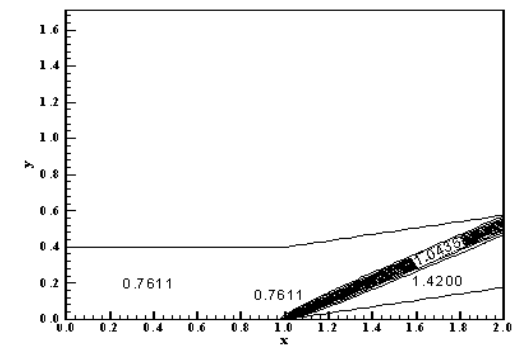
Figure 19: Pressure Contours (Mac).
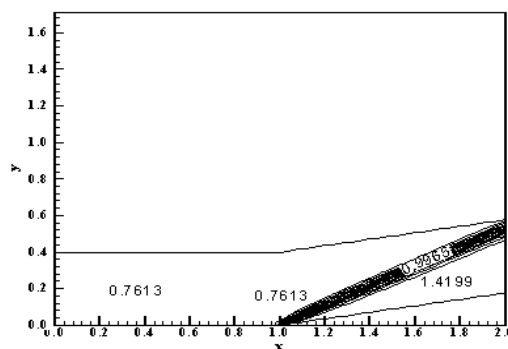
Figure 20: Pressure Contours (FPP).
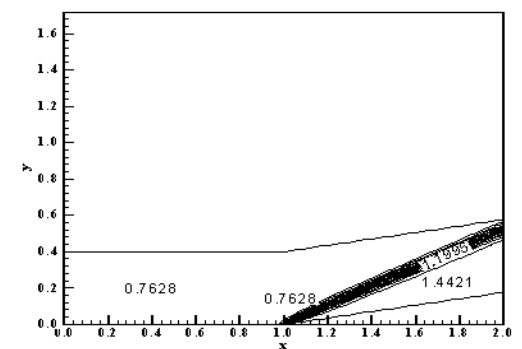
Figure 21: Pressure Contours (LS).
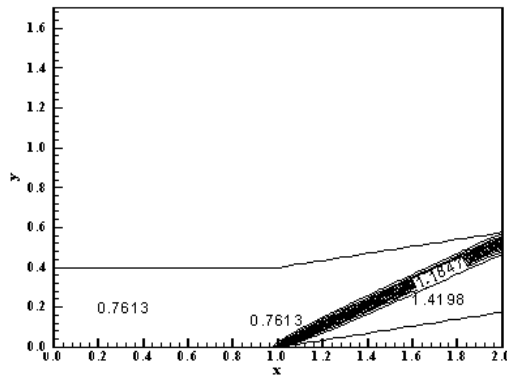
Figure 22: Pressure Contours (RK).
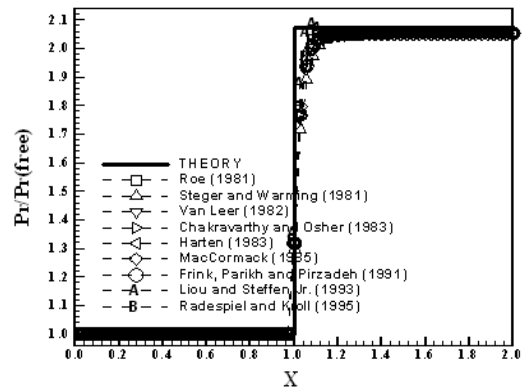
Figure 23: Wall Pressure Distributions (Imp).

Figure 23 shows the wall pressure distributions generated by all the studied schemes in this work, to the implicit case. They are compared with the oblique shock wave theory. All solutions present a smooth behavior typical of first order schemes, except the Liou and Steffen Jr. (1993) first order scheme, which present a peak at the beginning of the compression corner. Even so, all solutions capture the shock discontinuity using three cells. All solutions slightly underpredict the shock plateau. The best wall pressure distribution obtained in this implicit case is due to the Radespiel and Kroll (1995) first order algorithm.

Analyzing the oblique shock wave angle, using a transfer in Figures 14 to 22, it is possible to obtain the values of β to each scheme, as well the respective errors, shown in Tab. 2. As can be observed, the Steger and Warming (1981), the MacCormack (1985) and the Frink, Parikh and Pirzadeh (1991) first order schemes have yielded the best result. Errors less than 5.10% were observed.

Algorithm:	β (°):	Error (%):
Roe (1981)	28.8	4.73
Steger and Warming (1981)	28.0	1.82
Van Leer (1982)	28.5	3.64
Chakravarthy and Osher (1983)	28.5	3.64
Harten (1983)	28.5	3.64
MacCormack (1985)	28.0	1.82
Frink, Parikh and Pirzadeh (1991)	28.0	1.82
Liou and Steffen Jr. (1993)	28.2	2.55
Radespiel and Kroll (1995)	28.9	5.09

Table 2: Shock angle and percentage errors to the compression corner problem (Implicit case).

As conclusion, the explicit result of Harten (1983) first order scheme, with an error of 1.45%, has presented the best solution considering explicit and implicit ones.

6.3 Numerical data of the simulations

Table 3 presents the numerical data of the explicit simulations, involving maximum CFL number employed in the simulation by each scheme, iterations to convergence and computational cost of each scheme. The cheapest scheme is the Liou and Steffen Jr. (1993) first order scheme, whereas the most expensive scheme is the Frink, Parikh and Pirzadeh (1991) first order scheme. The former is 1,853.13% cheaper than the latter.

Algorithm:	CFL:	Iterations:	Cost[1]:
Roe (1981)	0.9	453	0.0000059
Steger and Warming (1981)	0.9	446	0.0000066
Van Leer (1982)	0.9	449	0.0000040
Chakravarthy and Osher (1983)	0.9	450	0.0000322
Harten (1983)	0.9	471	0.0000069
MacCormack (1985)	0.9	466	0.0000476
Frink, Parikh and Pirzadeh (1991)	2.6	161	0.0000625
Liou and Steffen Jr. (1993)	0.9	457	0.0000032
Radespiel and Kroll (1995)	0.9	453	0.0000039

[1]: Measured in seconds/per cell/per iteration.

Table 3: Numerical data of the explicit simulations.

Table 4 presents the numerical data of the implicit simulations, considering the same parameters evaluated in Tab. 3. The cheapest scheme is the Radespiel and Kroll (1995) first order scheme, whereas the most expensive scheme is the MacCormack (1985) first order scheme. The former is 223.93% cheaper than the latter. All algorithms presented significant values of CFL number in the implicit simulations. The minimum value employed, the worst case, was 3.0 (three) by the Van Leer (1982) first order scheme, but the gain in terms of convergence rate was approximately 209.66%. It is also important to emphasize the large CFL number employed by the implicit MacCormack (1985) first order scheme, achieving convergence in 28 iterations. The gain in terms of convergence rate was 1,564.29%. In other words, a relaxation procedure yields best gains in terms of convergence rate than an ADI procedure, because of the absence of the factorization error. On the other hand, the computational cost severely increases.

Algorithm:	CFL:	Iterations:	Cost[1]:
Roe (1981)	5.5	84	0.0000493
Steger and Warming (1981)	3.5	126	0.0000352
Van Leer (1982)	3.0	145	0.0000347
Chakravarthy and Osher (1983)	6.0	82	0.0000721
Harten (1983)	4.5	101	0.0000469
MacCormack (1985)	44.0	28	0.0001056
Frink, Parikh and Pirzadeh (1991)	5.5	84	0.0000528
Liou and Steffen Jr. (1993)	4.5	108	0.0000329
Radespiel and Kroll (1995)	3.5	127	0.0000326

[1]: Measured in seconds/per cell/per iteration.

Table 4: Numerical data of the implicit simulations.

Table 5 shows the comparison between the explicit and implicit computational costs of each scheme and the increase due to passing from the former to the latter. As can be observed the increase in the computational cost of the numerical schemes varies from 122% to 928%. It is important to highlight the decrease in the computational cost of the Frink, Parikh and Pirzadeh (1991) first order scheme as passing from implicit to the implicit case. As observed in Maciel (2011a), such behavior is due to the use of a Runge-Kutta method of five stages in the explicit case, which damages severely the computational cost of the explicit scheme. As

emphasized in Maciel (2011a), the implicit formulation is well optimized, which guarantees a reduction in the implicit computational cost in relation to its explicit counterpart. The minus signal is to highlight the reduction in the computational cost.

Algorithm:	Cost[(1)]/Exp:	Cost[(1)]/Imp:	Increase (%):
Roe (1981)	0.0000059	0.0000493	735.59
Steger and Warming (1981)	0.0000066	0.0000352	433.33
Van Leer (1982)	0.0000040	0.0000347	767.50
Chakravarthy and Osher (1983)	0.0000322	0.0000721	123.91
Harten (1983)	0.0000069	0.0000469	579.71
MacCormack (1985)	0.0000476	0.0001056	121.85
Frink, Parikh and Pirzadeh (1991)	0.0000625	0.0000528	-18.37
Liou and Steffen Jr. (1993)	0.0000032	0.0000329	928.13
Radespiel and Kroll (1995)	0.0000039	0.0000326	735.90

[(1)]: Measured in seconds/per cell/per iteration.

Table 5: Comparison of the explicit and implicit computational costs.

7 CONCLUSIONS

In this work, the Roe (1981), the Steger and Warming (1981), the Van Leer (1982), the Chakravarthy and Osher (1983), the Harten (1983), the MacCormack (1985), the Frink, Parikh and Pirzadeh (1991), the Liou and Steffen Jr. (1993) and the Radespiel and Kroll (1995) first order schemes are implemented employing an implicit formulation to solve the Euler equations in two-dimensions. These schemes are implemented according to a finite volume formulation and using a structured spatial discretization. The Roe (1981), the Chakravarthy and Osher (1983), the Harten (1983) and the Frink, Parikh and Pirzadeh (1991) schemes are flux difference splitting ones, whereas the others are flux vector splitting schemes. The implicit schemes employ an ADI approximate factorization or Symmetric Line Gauss-Seidel to solve implicitly the Euler equations. Explicit and implicit results are compared, as also the computational costs, trying to emphasize the advantages and disadvantages of each formulation. The schemes are accelerated to the steady state solution using a spatially variable time step, which has demonstrated effective gains in terms of convergence rate (Maciel, 2005). The algorithms are applied to the solution of the physical problem of the supersonic flow along a compression corner.

The results have demonstrated that the most accurate solutions are obtained with the Harten (1983) first order scheme, when implemented in its explicit version. The best wall pressure distribution is obtained by the Radespiel and Kroll (1995) first order scheme, in both explicit and implicit cases. All algorithms present solutions free of oscillations, under- or overshoot in the pressure contours and in the wall pressure distribution. Only the Liou and Steffen Jr. (1993) first order scheme presents a pressure peak at the beginning of the compression corner. In both explicit and implicit cases, the shock discontinuity is captured within three cells by all algorithms. All schemes estimate the shock angle of the oblique shock wave with errors less than 5.10% in both explicit and implicit solutions. The best solution, involving explicit and implicit simulations, is due to the explicit Harten (1983) scheme.

As can be observed from Table 3, the cheapest scheme, in its explicit version, is due to the Liou and Steffen Jr. (1993) first order scheme, whereas the most expensive scheme is due to the Frink, Parikh and Pirzadeh (1991) first order scheme. The former is 1,853.13% cheaper

than the latter. From Table 4, its implicit counterpart, the cheapest scheme is due to the Radespiel and Kroll (1995) first order scheme, whereas the most expensive scheme is due to the MacCormack (1985) first order scheme. The Radespiel and Kroll (1995) scheme is 223.93% cheaper than the MacCormack (1985) scheme. It is important to highlight the significant gain in terms of convergence rate when using the MacCormack (1985) first order scheme, as passing from explicit to implicit implementation. This gain is estimated in 1,564.29%, which is very encouraging, although the high computational cost of the implicit implementation deserves special attention.

Another important consideration taking into account Tab. 5 is the great increase in the computational cost involving the same variant of a numerical scheme when passing from explicit to implicit implementation. The Liou and Steffen Jr. (1993) first order scheme presents the biggest increase in the computational cost involving all schemes (about 928%), but it is important to note that all schemes suffer an increase of no minimal 122% when passing from explicit to implicit formulation, which means a great penalty to improve the numerical results. In the present study, this penalty was not accepted because the best estimative of the shock angle was obtained with the explicit version of the Harten (1983) first order scheme. Moreover, no meaningful gains in terms of the improvement in the capture of the shock discontinuity by each scheme was achieved because the same number of cells – three – was obtained in both explicit and implicit cases. Hence, the author concludes that an explicit formulation yields satisfactory behavior in the capture of shock discontinuities.

REFERENCES

Anderson Jr., J. D., *Fundamentals of Aerodynamics*. McGraw-Hill, Inc., EUA, 563p, 1984.

Beam, R. M., and Warming, R. F., An Implicit Factored Scheme for the Compressible Navier-Stokes Equations. *AIAA Journal*, 16(4): 393-402, 1978.

Chakravarthy, S. R., and Osher, S., Numerical Experiments with the Osher Upwind Scheme for the Euler Equations. *AIAA Journal*, 21(9): 1241-1248, 1983.

Douglas, J., On the Numerical Integration of $u_{xx}+u_{yy}=u_t$ by Implicit Methods. *Journal of the Society of Industrial and Applied Mathematics*, 3: 42-65, 1955.

Douglas, J., and Gunn, J. E., A General Formulation of Alternating Direction Methods. *Numerische Mathematiks*, 6: 428-453, 1964.

Frink, N. T., Parikh, P., and Pirzadeh, S., Aerodynamic Analysis of Complex Configurations Using Unstructured Grids. *AIAA 91-3292-CP*, 1991.

Harten, A., High Resolution Schemes for Hyperbolic Conservation Laws. *Journal of Computational Physics*, 49: 357-393, 1983.

Jameson, A., and Mavriplis, D. J., Finite Volume Solution of the Two-Dimensional Euler Equations on a Regular Triangular Mesh", *AIAA Journal*, 24(4): 611-618, 1986.

Kutler, P., Computation of Three-Dimensional, Inviscid Supersonic Flows. *Lecture Notes in Physics*, 41: 287-374, 1975.

Liou, M., and Steffen Jr., C. J., A New Flux Splitting Scheme. *Journal of Computational Physics*, 107: 23-39, 1993.

MacCormack, R. W., An Introduction and Review of the Basics of Computational Fluid Dynamics. *Lecture Notes*, University of Washington, Seattle, Washington, EUA, 1984.

MacCormack, R. W., Current Status of Numerical Solutions of the Navier-Stokes Equations. *AIAA Paper 85-0032*, 1985.

Maciel, E. S. G., *Simulação Numérica de Escoamentos Supersônicos e Hipersônicos Utilizando Técnicas de Dinâmica dos Fluidos Computacional*. PhD thesis, ITA, CTA, São

José dos Campos, SP, Brazil, 258 p, 2002.

Maciel, E. S. G., Analysis of Convergence Acceleration Techniques Used in Unstructured Algorithms in the Solution of Aeronautical Problems – Part I. *Proceedings of the XVIII International Congress of Mechanical Engineering (XVIII COBEM)*, Ouro Preto, MG, Brazil, 2005.

Maciel, E. S. G., Comparison Among the First Order Upwind Algorithms of Roe, of Steger and Warming, of Van Leer and of Chakravarthy and Osher in the Solution of the Euler Equations in 2D – Theory. *Proceedings of the 8th Symposium of Computational Mechanics (VIII SIMMEC)*, Belo Horizonte, MG, Brazil, 2008a.

Maciel, E. S. G., Comparação Entre Algoritmos de Separação de Vetores de Fluxo e de Diferenças de Fluxo de Primeira Ordem na Solução das Equações de Euler em Duas Dimensões – Teoria. *Proceedings of the Primer Congreso Argentino de Ingeniería Mecánica (I CAIM)*, Bahía Blanca, Argentina, 2008b.

Maciel, E. S. G., Extension of the Steger and Warming and Radespiel and Kroll Algorithms to Second Order Accuracy and Implicit Formulation Applied to the Euler Equations in Two-Dimensions – Results. *Proceedings of the VI National Congress of Mechanical Engineering (VI CONEM)*, Campina Grande, PB, Brazil, 2010.

Maciel, E. S. G., Extension of Frink, Parikh and Pirzadeh and Liou and Steffen Jr. Algorithms to Second Order Accuracy and Implicit Formulations Applied to the Euler Equations in Two-Dimensions – Results. *Proceedings of the XXI International Congress of Mechanical Engineering (XXI COBEM)*, Natal, Rio Grande do Norte, Brazil, 2011a.

Maciel, E. S. G., Extension of the Roe and Van Leer Algorithms to Second Order Accuracy and Implicit Formulations Applied to the Euler Equations in Two-Dimensions. *Anales del XIX Congreso sur Métodos Numéricos y sus Aplicaciones (XIX ENIEF)*, Rosario, Argentina, 2011b.

Peaceman, D. W., and Rachford, H. H., The Numerical Solution of Parabolic and Elliptic Differential Equations. *Journal of the Society of Industrial and Applied Mathematics*, 3: 28-41, 1955.

Radespiel, R., and Kroll, N., Accurate Flux Vector Splitting for Shocks and Shear Layers. *Journal of Computational Physics*, 121: 66-78, 1995.

Roe, P. L., Approximate Riemann Solvers, Parameter Vectors, and Difference Schemes. *Journal of Computational Physics*, 43: 357–372, 1981.

Steger, J. L., and Warming, R. F., Flux Vector Splitting of the Inviscid Gasdynamic Equations with Application to Finite-Difference Methods. *Journal of Computational Physics*, 40: 263-293, 1981.

Van Leer, B., Flux-Vector Splitting for the Euler Equations. *Proceedings of the 8th International Conference on Numerical Methods in Fluid Dynamics*, E. Krause, Editor, Lecture Notes in Physics, 170: 507-512, Springer-Verlag, Berlin, 1982.

Yee, H. C., Warming, R. F., and Harten, A., Implicit Total Variation Diminishing (TVD) Schemes for Steady-State Calculations. *Journal of Computational Physics*, 57: 327-360, 1985.